Materials Today Bio 12 (2021) 100161

Contents lists available at ScienceDirect

Materials Today Bio

journal homepage: www.journals.elsevier.com/materials-today-bio

Methoxy polyethylene glycol modification promotes adipogenesis by inducing the production of regulatory T cells in xenogeneic acellular adipose matrix

Kaiyang Liu [1], Yunfan He [1], Yao Yao, Yuchen Zhang, Zihan Cai, Jiangjiang Ru, Xiangdong Zhang, Xiaoxuan Jin, Mimi Xu, Yibao Li, Qizhuan Ma, Jianhua Gao **, Feng Lu *

Department of Plastic and Cosmetic Surgery, Nanfang Hospital, Southern Medical University, Guangzhou, Guangdong, People's Republic of China

ARTICLE INFO

Keywords:
Acellular adipose matrix
Xenotransplantation
Methoxy polyethylene glycol
Regulatory T cell
Adipogenesis

ABSTRACT

Acellular adipose matrix (AAM) has emerged as an important biomaterial for adipose tissue regeneration. Current decellularization methods damage the bioactive components of the extracellular matrix (ECM), and the residual immunogenic antigens may induce adverse immune responses. Here, we adopted a modified decellularization method which can protect more bioactive components with less immune reaction by methoxy polyethylene glycol (mPEG). Then, we determined the adipogenic mechanisms of mPEG-modified AAM after xenogeneic transplantation. AAM transplantation caused significantly lesser adipogenesis in the wild-type group than in the immune-deficient group. The mPEG-modified AAM showed significantly lower immunogenicity and higher adipogenesis than the AAM alone after xenogeneic transplantation. Furthermore, mPEG modification increased regulatory T (Treg) cell numbers in the AAM grafts, which in turn enhanced the M2/M1 macrophage ratio by secreting IL-10, IL-13, and TGF-β1. These findings suggest that mPEG modification effectively reduces the immunogenicity of xenogeneic AAM and promotes adipogenesis in the AAM grafts. Hence, mPEG-modified AAM can serve as an ideal biomaterial for xenogeneic adipose tissue engineering.

1. Introduction

The reconstruction of soft tissue defects caused by traumatic injuries, surgical approaches (i.e., mastectomy) or congenital anomalies is a major challenge in plastic surgery. Generally, plastic surgeons use autologous tissue flap transfer to repair soft tissue defects [1,2]. However, donor-site morbidity and the tenuous nature of microsurgical tissue transfer makes it a complex operative procedure that requires an adequately trained surgeon. Autologous fat grafting is a common technique for soft tissue reconstruction; however, its clinical effectiveness is often plagued by unpredictable outcomes, fat necrosis and oil-cyst formation [3,4]. Various types of naturally-derived biopolymers and synthetic polymers have been used to fill soft tissue defects. However, these materials may not able to integrate with the surrounding tissues and induce adipogenesis, thus being rapidly absorbed *in vivo* [5]. Therefore, adipose tissue reconstruction has emerged as a new strategy to overcome the difficulties associated with plastic surgery.

In the recent decade, acellular adipose matrix (AAM) has attracted considerable attention for soft tissue reconstruction owing to its abundant sources and potential to spontaneously induce adipogenesis *in vivo* [6–8]. However, AAM failed to induce significant adipogenesis in animal experiments, especially in xenogeneic transplant models [9,10]. Moreover, a recent clinical application study showed that adipogenesis could only be observed in the peripheral portion of allogeneic AAM grafts [11]. Matrix-bound bioactive components (i.e., growth factors and bioactive peptides) of extracellular matrix (ECM) biomaterials were recently found

* Corresponding author. Department of Plastic and Cosmetic Surgery, Nanfang Hospital, Southern Medical University, 1838 Guangzhou North Road, Guangzhou, Guangdong, 510515, People's Republic of China.
** Corresponding author.
E-mail addresses: liuky0510@hotmail.com (K. Liu), doctorheyunfan@hotmail.com (Y. He), doctoryaoyao@hotmail.com (Y. Yao), zhangyc0123@hotmail.com (Y. Zhang), tsaizh@foxmail.com (Z. Cai), malaria1999@hotmail.com (J. Ru), ZhangXD0105@hotmail.com (X. Zhang), Jinxiaoxuan0110@hotmail.com (X. Jin), Xumimi1125@hotmail.com (M. Xu), doctorliyibao@hotmail.com (Y. Li), drcjma@icloud.com (Q. Ma), doctorgaojianhua@outlook.com (J. Gao), doctorlufeng@hotmail.com (F. Lu).
[1] Contributed equally to this paper.

https://doi.org/10.1016/j.mtbio.2021.100161
Received 14 August 2021; Received in revised form 16 November 2021; Accepted 17 November 2021
Available online 19 November 2021

to play major roles in directing cell fate and inducing tissue regeneration [12–14]. These ECM components create a niche that can dynamically regulate the behaviour of stem/progenitor cells, provide extracellular clues for cell recruitment, and support cell differentiation into functional tissues [15,16]. However, the current decellularization strategies generally involve lengthy chemical and enzymatic treatments, which inevitably destroy the bioactive components of the ECM and adversely affect the *in vivo* regeneration of the AAM [17–19]. In addition, it is difficult to completely remove all immunogenic antigens using the current decellularization methods [20–22]. The residual antigens may cause an adverse immune response *in vivo*, which is another important factor that limits the adipogenesis caused by xenogeneic AAM [21,23]. Therefore, an alternative strategy that can maximise the retention of ECM bioactive components and minimise the unwanted immune reactions would be highly desirable.

The immunocamouflage technique has emerged as a promising approach to modify immunogenic antigens [24,25]. Methoxy polyethylene glycol (mPEG) is an effective, non-toxic, and non-immunogenic material for the immunocamouflage of cell surfaces, which has been approved by the Food and Drug Administration [26]. mPEG can reduce or prevent host immune rejection through mPEG-induced charge and steric camouflage by covalently binding to the amino acid residues on the cell surface [24,27]. In the past decade, mPEG has been used to bind the surfaces of allogeneic transplanted cells (e.g., erythrocytes, pancreatic β cells and leukocytes) and corneal grafts to suppress host immune rejection and prolong the functions of the transplants [24,25,28,29]. However, few studies have been conducted on the mPEG modification of the AAM grafts. Thus, we hypothesise that mPEG modification can suppress the immunogenicity and promote the adipogenesis of xenogeneic AAM.

To verify this hypothesis, xenotransplant animal models were constructed to explore the impact of mPEG modification on the adipogenesis of xenogeneic AAM. mPEG was introduced to modify the residual antigens in the AAM grafts, and the safety and immunocamouflage efficiency of mPEG modification on AAM were assessed both *in vitro* and *in vivo*. In addition, the adipogenesis mechanisms of mPEG-modified AAM after xenogeneic transplantation were investigated.

2. Materials and methods

2.1. Animal models

The experimental mice were supplied by the Southern Medical University Laboratory Animal Centre, and house in microisolator cages at the Animal Experiment Centre of Nanfang Hospital. All experiments were performed in accordance with the guidelines of the National Institutes of Health guide for the care and use of Laboratory animals. Ethical approval for this study was obtained from the Nanfang Hospital Animal Ethics Committee Laboratory, Southern Medical University, China.

2.2. Preparation of AAM

After obtaining informed consent, human adipose tissues were collected from the female patients who underwent abdominal liposuction. The adipose tissues were decellularized according to the methods published by He et al. [30] and Kokai et al. [11]. Briefly, the lipoaspirate was subjected to 3 cycles of freezing and thawing (−80 to 37 °C). Following centrifugation (2000×*g*, 3 min), the substratum samples were homogenised at 30,000 rpm for 1 min. The adipose suspension was collected and then centrifuged at 3000×*g* for 3 min. The lipid-depleted adipose tissues were decellularized prior to a 6-hr polar solvent extraction in 99.9% isopropanol. After rinsing three times with PBS, the samples were mixed with aqueous sodium deoxycholate and agitated for 12 h. Finally, the samples were disinfected with 0.1% peracetic acid in 4% ethanol for 4 h. The resulting AAM was kept at −80 °C.

2.3. mPEG modification of AAM

The mPEG solution (3% w/v) was prepared by dissolving mPEG succinimidyl propionate 5KD (Seebio, 281,100, China) in alkaline PBS (Leagene, R22127, China; pH 7.88). To produce mPEG-modified AAM, the mPEG solution was used to immerse AAM at 25 °C for 1 h. Subsequently, the mPEG-modified AAM was rinsed twice with PBS, centrifuged (2500×*g*, 3 min) to remove the supernatant, and then stored until further analysis.

2.4. Antigen detection of mPEG-modified AAM and cell viability assay

The sections were stained using antibodies against major histocompatibility complex (MHC) antigen class I (MCH-I, Santa Cruz Biotechnology, sc-55582, CA, USA) and MHC antigen class II (MHC-II, Abcam, ab170867, UK). Human adipose-derived stromal cells (hASCs) were supplied by Cyagen Biosciences (Cyagen, HUXMD-01001, China). The hASCs (approximately 5×10^5 per well) were grown with/without 3% (w/v) mPEG succinimidyl propionate in culture medium (Cyagen, HUXMD-90011, China) for three days at 37 °C with 5% CO_2. One millilitre of PBS solution supplemented with 2 μL of 1 mg/mL calcein-AM (AnaSpec, CA, USA) and 2 μL of 1 mg/mL 4′,6-diamidino-2-phenylindole (DAPI) (Sigma, USA) were pipetted into each well, and then incubated for 10 min at 37 °C. Live and dead cells were counted from images taken with a fluorescence microscope (BX 51, Olympus).

2.5. Xenotransplantation models

The mice were categorized into three groups: immune-deficient group, xenotransplantation group, and xenotransplantation (mPEG-modified) group. After anaesthesia by intraperitoneally injecting 50 mg/kg pentobarbital sodium, the subcutaneously bilateral dorsal regions were selected as the transplant sites. In the immune-deficient and xenotransplantation groups, 0.25 mL/side AAM was transplanted into BALB/c nude mice and BALB/c mice, respectively. In the xenotransplantation (mPEG-modified) group, 0.25 mL/side mPEG-modified AAM was transplanted into BALB/c mice. Both AAM and mPEG-modified AAM were sheared under aseptic conditions and then injected into the mice using an 18-gauge needle. The animals were sacrificed at week 1, 4 and 12 (n = 5 per group at each time point). The tissue samples were harvested, and the volume of fluid displacement was measured to obtain the graft volume. Half of the sample was immediately used for fluorescence-activated cell sorting. A quarter of the sample was fixed in 4% paraformaldehyde for histological and immunofluorescence staining. The remaining sample was preserved at −80 °C for real-time PCR assay and Western blot assay.

2.6. Immunofluorescence staining of the harvested samples

After embedding in paraffin, the samples were sectioned and then subjected to immunofluorescence staining. Briefly, the sections were incubated with the following primary antibodies: rabbit anti-mouse CD206 (Abcam, ab64693, UK), rabbit anti-mouse Foxp3 (Abcam, ab215206, UK), rat anti-mouse Mac2 (Cedarlane, CL8942AP, Canada) and guinea pig anti-mouse Perilipin (Progen, GP29, Germany), followed by the corresponding secondary antibodies. After DAPI staining (Sigma, D9542, USA), the sections were observed and photographed using a FV10i-W confocal laser scanning microscope (Olympus, Japan).

2.7. Immunoglobulin expression in blood samples

Blood samples were collected from the orbital sinus of BALB/c mice in xenotransplantation and xenotransplantation (mPEG-modified) groups at week 1, 4 and 12 (n = 5 per group at each time point). After centrifugation (1200×*g*, 10 min, 4 °C), the supernatant was aliquoted and kept at −80 °C. Mouse IgG (MM-0057 M, China) and mouse IgM ELISA Kit (MM-0058 M, China) enzyme-linked immunosorbent assay (ELISA) kits were

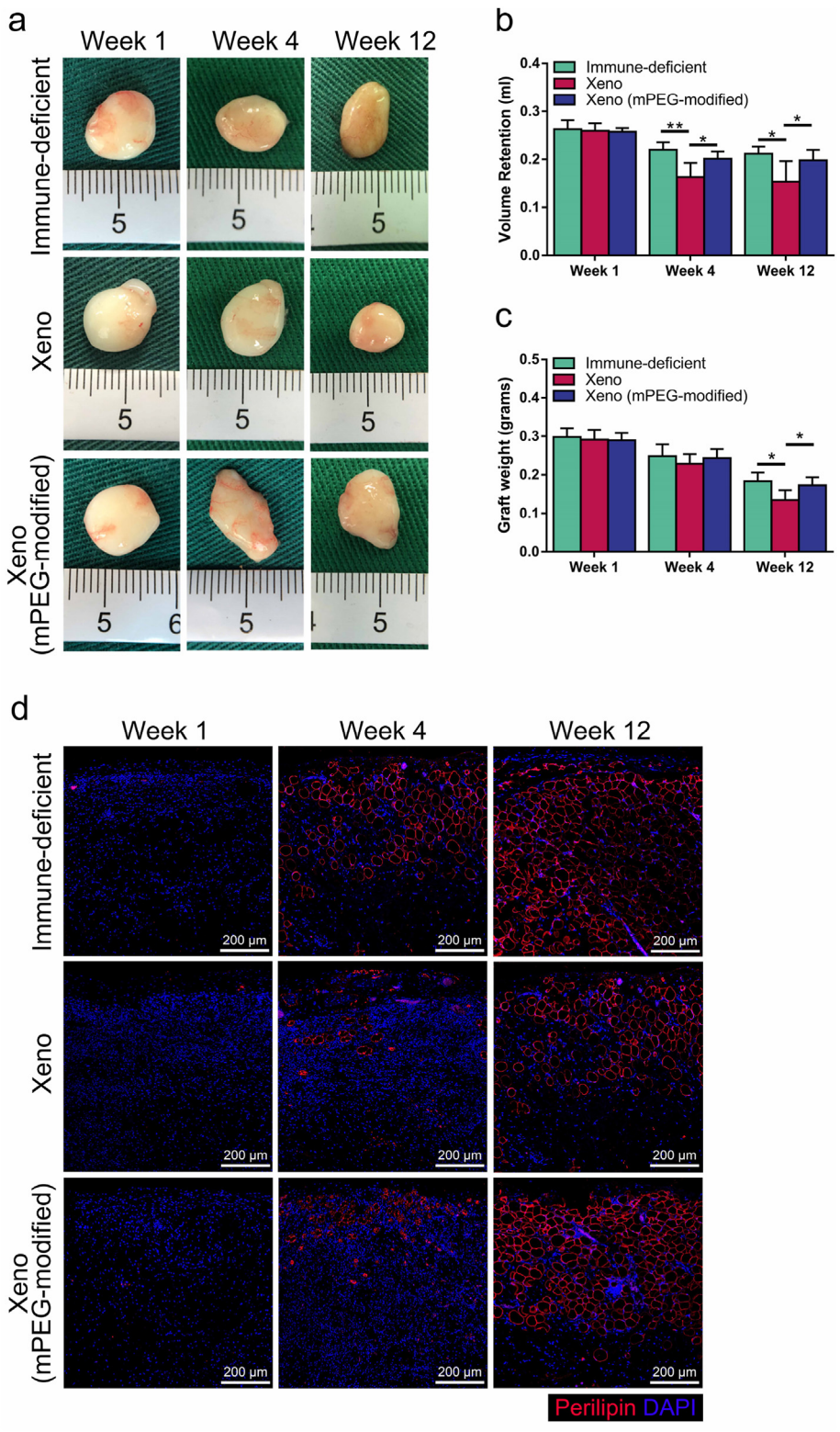

Fig. 1. The gross view, volume retention rate and histology of the AAM grafts. (a) Representative gross view of the transplanted grafts in the immune-deficient group, xenotransplantation group, and xenotransplantation (mPEG-modified) group at week 1, 4 and 12. (b) Quantification of the graft volume retention in the three groups. (c) Quantification of the graft weight in the three groups. (d) Representative immunofluorescence staining (perilipin) of the transplanted grafts in the three groups at week 1, 4, and 12. Scale bar = 200 μm * = $p < 0.05$, ** = $p < 0.01$.

used to assess the expression of IgG and IgM in plasma, respectively, as per the manufacturer's protocols.

2.8. Fluorescence-activated cell sorting (FACS)

The heparinised whole blood was withdrawn from the mouse orbital sinus. Red blood cells were isolated with Easy Lyse Solution (10 mL; Leinco Technologies, USA), and then stained with Foxp3-PE, CD4-FITC, IL17A-APC, IFN-γ-Pacific Blue, IL4-PE, CD3-FITC and CD8-Pacific Blue (BioLegend, CA, USA). For graft analysis, the graft samples were homogenised and digested with collagenase (0.125%; Sigma, Missouri, USA) in a shaking water bath at 37 °C for 30 min. After centrifugation (800×*g*, 3 min) and resuspension, the cells were stained with the following monoclonal antibodies: CD11b-Pacific Blue, CD11c-PE/Cy7, Foxp3-PE, F4/80-PE, CD206-FITC CD4-FITC, IL17A-APC, IFN-γ-Pacific Blue, IL4-PE, CD3-FITC, and CD8-Pacific Blue (BioLegend, CA, USA). An irrelevant control

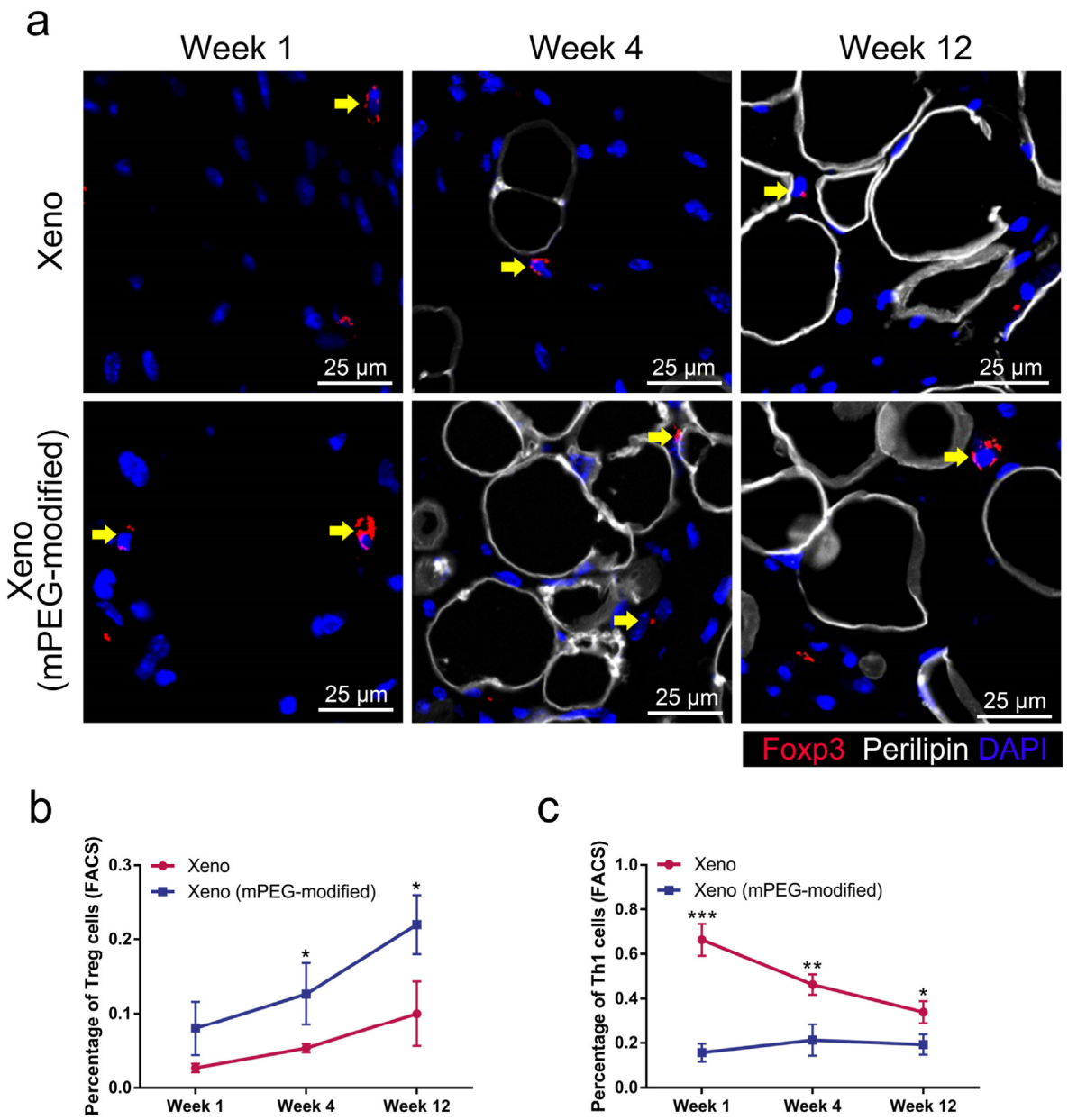

Fig. 2. Immunofluorescence staining and FACS results of T cells in the AAM grafts. (a) Foxp3 immunofluorescence staining of Treg cells (yellow arrow) in the mPEG-modified xenotransplantation and control xenotransplantation groups at week 1, 4 and 12. (b and c) FACS analysis of Treg cells and Th1 cells in the two groups at week 1, 4 and 12. Scale bar = 100 μm * = $p < 0.05$, ** = $p < 0.01$, *** = $p < 0.001$.

monoclonal antibody was included for each fluorochrome. Finally, the cells were analysed using a BD LSR-II flow cytometer (Becton Dickinson, CA, USA). Cell Quest software (Becton Dickinson, CA, USA) was employed for data acquisition and analysis. A gate was set to exclude 99.9% of the isotype control-labelled cells.

2.9. Lymphocyte co-culture assay

The spleen from eight-week-old BALB/c mice was isolated, mashed up on a 70-μm cell strainer using the plunger end of a syringe, and then rinsed with DMEM (GIBCO, 11995500BT, USA) containing 10% FBS (GIBCO, 10099141-S, USA). After centrifugation (800×*g*, 3 min), the cell suspensions were diluted with DMEM containing 10% FBS to a final concentration of 1×10^5 cells/mL. Spleen lymphocytes (2 mL) alone served as a control group. Spleen lymphocytes (2 mL) co-cultured with 0.5 mL AAM and mPEG-modified AAM served as the AAM and mPEG-modified AAM groups, respectively. After 3 days of incubation at 37 °C with 5% CO_2, the cells were filtered through the cell strainer for FACS and Western blot assays.

2.10. Treg cell regulation in BALB/c mice

BALB/c mice were categorized into three groups: anti-CD25 antibody treatment group (a decrease in Treg cell counts), CD28-SA treatment group (an increase in Treg cell counts), and control group. The anti-CD25 antibody treatment group and CD28-SA treatment group were treated with anti-CD25 monoclonal antibody (250 μg; clone PC61; BioLegend, CA, USA) and superagonistic anti-CD28 monoclonal antibody (200 μg; clone D665; Biocompare, CA, USA), respectively. All reagents were diluted with PBS (0.3 mL) and injected intraperitoneally 1 day before AAM grafting. The mice in control group were treated with 0.3 mL PBS. The AAM was sheared under aseptic conditions and then injected into the mice using an 18-gauge needle. The animals were sacrificed at week 1, 4 and 12 (n = 5 per group at each time point).

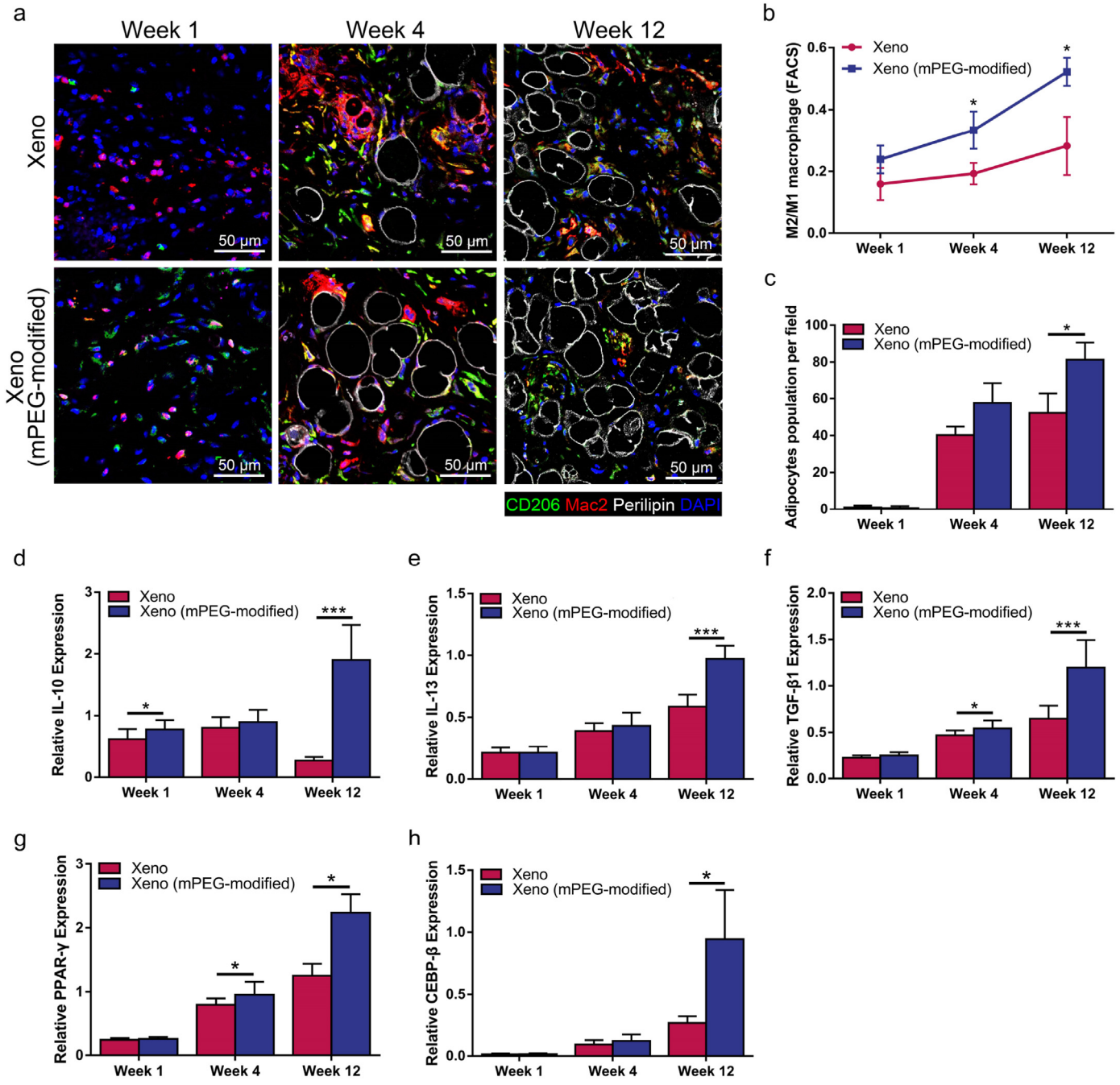

Fig. 3. Immunofluorescence staining and FACS results of the macrophages as well as the expression of associated cytokines and adipogenic marker genes in the AAM grafts. (a) Immunofluorescence staining of Mac2 and CD206 in the mPEG-modified xenotransplantation and control xenotransplantation groups at week 1, 4 and 12. (b) Quantification of M2/M1 macrophage (F4/80+, CD11b+, CD11c+, $CD206^{high}$/F480+, CD11b+, CD11c+, $CD206^{low}$) ratio in the two groups at week 1, 4 and 12. (c) Quantification of adipocyte cell number in the grafts of the two groups. (d–f) Real-time PCR measurements of M2 macrophage polarisation-associated cytokines (IL-10, IL-13 and TGF-β1) in the two groups. (g and h) Real-time PCR measurements of the adipogenic marker genes (PPAR-γ and CEBP-β) in the two groups. Scale bar = 100 μm * = $p < 0.05$, *** = $p < 0.001$.

2.11. Co-culture of Treg cells and M0 macrophages

Spleen lymphocytes from eight-week-old male C57BL/6 mice were harvested as described previously for the sorting of Treg cell subsets. Treg cells were sorted from the spleen lymphocytes using a Treg cell ISO kit (STEMCELL, #18783, Canada). To sort M0 macrophage cell subsets, mouse tibias and femurs were dissected and rinsed with serum-free RPMI 1640 (GIBCO, C11875500CP, USA). Lavage fluid was filtered through a 100-μm cell strainer, followed by centrifugation (500×*g*, 5 min). The cells were resuspended in RBC lysis buffer (Solarbio, R1010, China), and then incubated for 5 min at 4 °C. After centrifugation (500×*g*, 5 min, at 4 °C), the cells were harvested, washed and resuspended in RPMI 1640 culture medium containing 10% FBS, 2 mM L-glutamine (Solarbio, G0200, China), 10 mg/mL Gibco penicillin/streptomycin (GIBCO, 15140122, USA) and 100 μg/L granulocyte-macrophage colony-stimulating factor (PEPROTECH, 315-03-5, USA). After 3 days of incubation at 37 °C with 5% CO_2, M0 macrophages were transferred to a sterile tube, and counted. For co-culture assays, 2.5×10^5 M0 macrophages and gradient number of Treg cells (M0: 0 Treg/well; $Treg^{+}$: 1×10^4 Treg/well; $Treg^{++}$: 5×10^4 Treg/well; and Treg+++: 2.5×10^5 Treg/well)

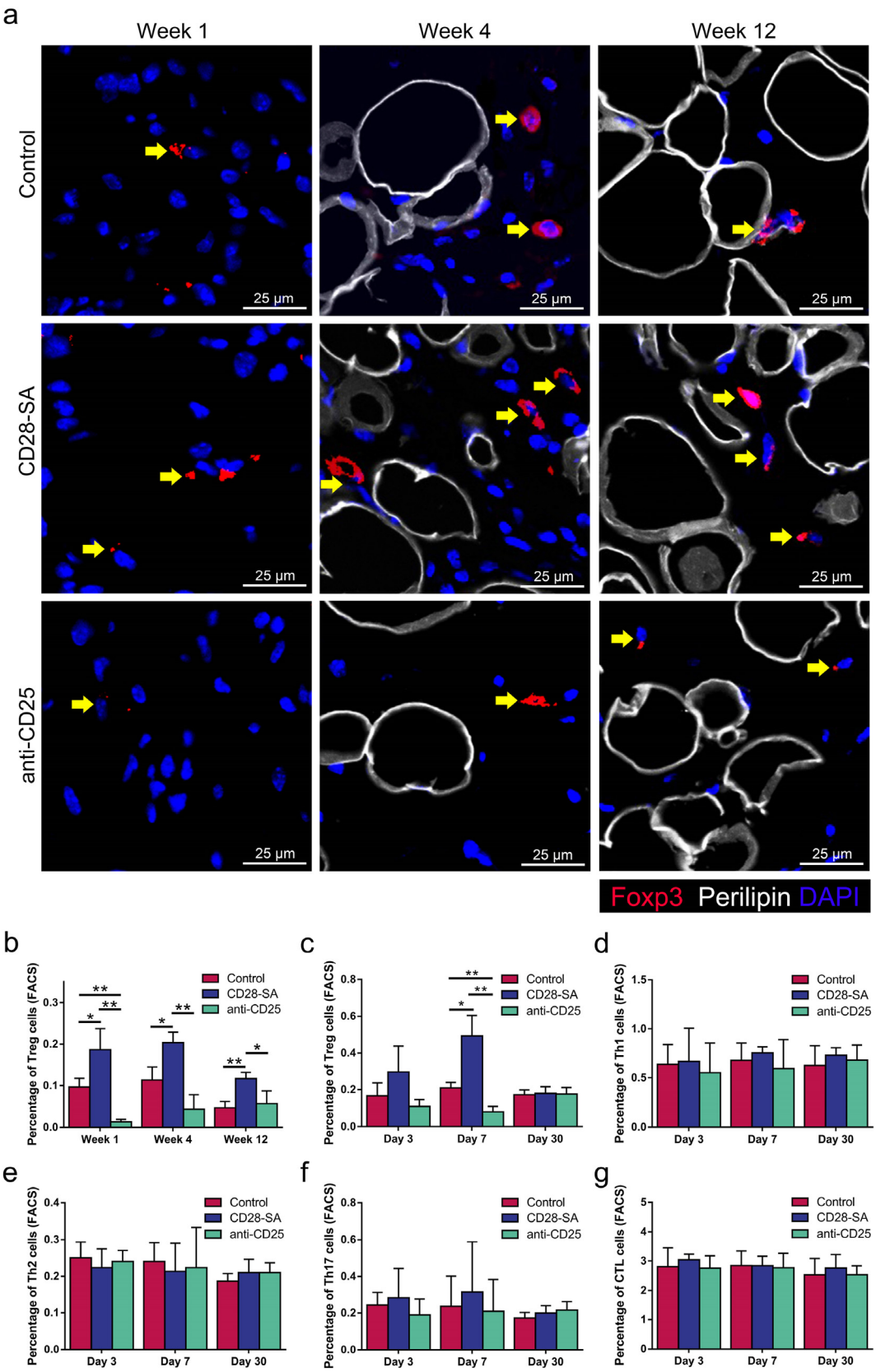

Fig. 4. Immunofluorescence staining and FACS results of the AAM grafts. (a) Foxp3 immunofluorescence staining of Treg cells (yellow arrow) in the control, CD28-SA treatment and anti-CD25 antibody treatment groups at week 1, 4 and 12. (b) FACS quantification of Treg cells in the three groups. FACS quantification of (c) Treg cells ($CD4^+$ and Foxp3+), (d) Th1 cells ($CD4^+$ and IFN-γ+), (e) Th2 cells ($CD4^+$ and IL-4+), (f) Th17 cells ($CD4^+$ and IL-17A+), and (g) cytotoxic T lymphocytes ($CD4^+$ and $CD8^+$) in the circulation at day 3, 7 and 30. Scale bar = 100 μm * = $p < 0.05$, ** = $p < 0.01$.

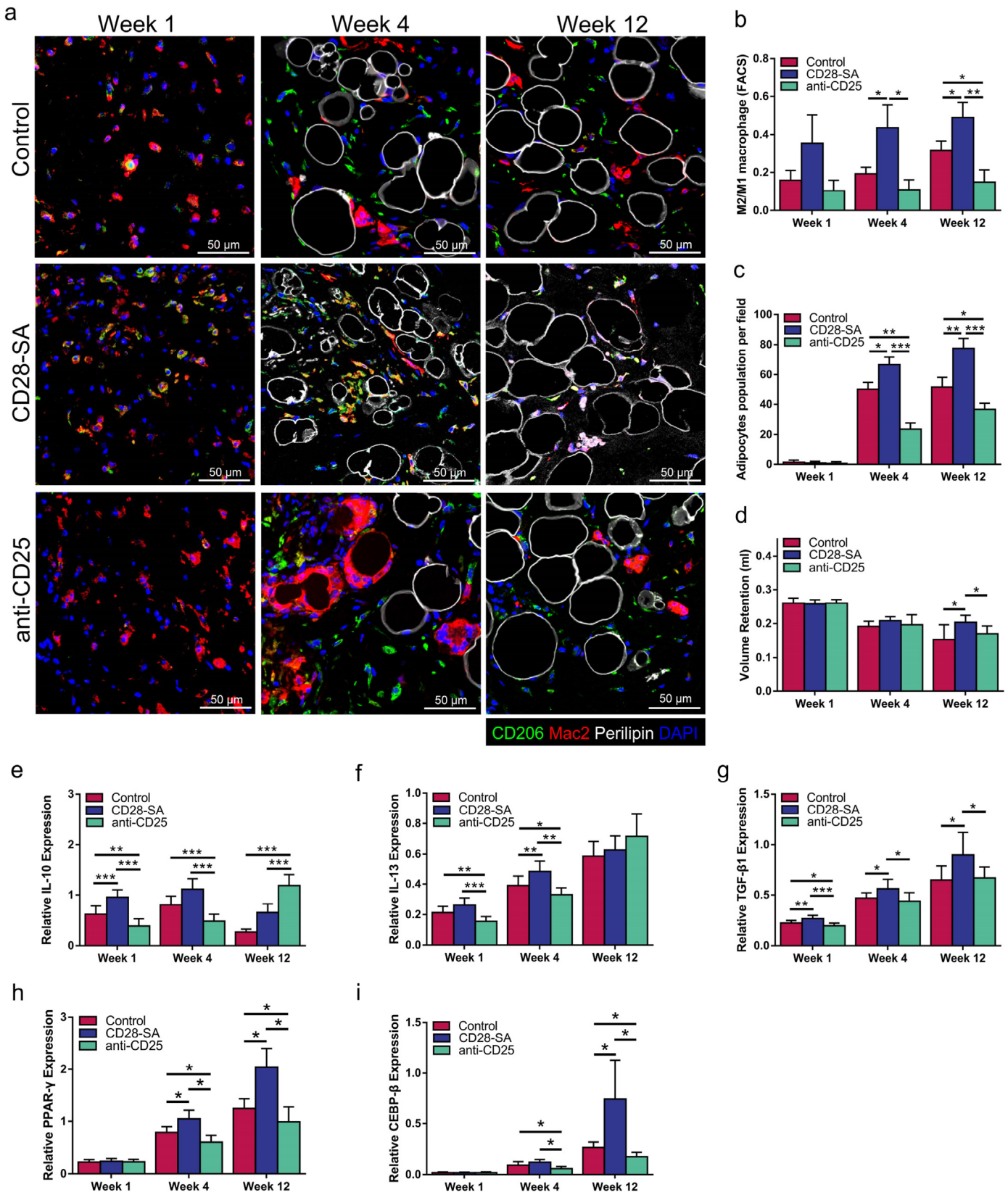

Fig. 5. Immunofluorescence staining of the macrophages as well as the expression of associated cytokines and adipogenic marker genes in the AAM grafts. (a) Immunofluorescence staining of Mac2 and CD206 in the control group, CD28-SA treatment group, and anti-CD25 antibody treatment group at week 1, 4 and 12. (b) FACS quantification of the M2/M1 macrophage (F4/80+, CD11b+, CD11c+, $CD206^{high}$/F480+, CD11b+, CD11c+, $CD206^{low}$) ratio of the three groups at week 1, 4 and 12. (c) Quantification of adipocytes in the AAM grafts of the three groups. (d) Quantification of graft volume retention in the three groups. (e–g) Relative mRNA expression levels of M2 macrophage polarisation-associated cytokines (IL-10, IL-13 and TGF-β1) in the AAM grafts. (h and i) Real-time PCR measurements of the adipogenic marker genes (PPAR-γ and CEBP-β) in the three groups. Scale bar = 100 μm * = $p < 0.05$, ** = $p < 0.01$, *** = $p < 0.001$.

were co-cultured with RPMI 1640 containing 10% FBS, 25 IU/mL recombinant murine IL-2 (PEPROTECH, 212-12-20, USA), and 10 mg/mL penicillin/streptomycin in mPEG-modified AAM for 5 days at 37 °C with 5% CO_2. The cells were harvested for FACS and Western blot assays.

2.12. Real-time PCR assay

The expression levels of PPAR-γ, CEBP-β, IL-10, IL-13 and TGF-β1 were quantified by real-time PCR (Applied Biosystems 7500, USA). The 2-ΔΔCt method was employed to calculate the relative expression level of each gene. The following primers were used: forward, GAACCTGCATCTCCACCTTATT and reverse, TGGAAGCCTGATGCTTTATCC for PPAR-γ; forward, CTTGATGCAATCCGGATCAAAC and reverse, CCCGCAGGAACATCTTTAAGT for CEBP-β; forward, CCCTTTGC TATGGTGTCCTTTC and reverse, AGGATCTCCCTGGTTTCTCTTC for IL-10; forward, CCTGGCTCTTGCTTGCCTT and reverse, GGTCTTGT GTGATGTTGCTCA for IL-13; and forward, CTTCAATACGTCAGACATTCGGG and reverse, GTAACGCCAGGAATTGTTGCTA for TGF-β1.

2.13. Statistical tests

Data were analysed using IBM SPSS (V22.0; IBM Corp., Armonk, NY, USA). An independent variable *t*-test was performed to compare the two mean values. For comparison of three or more means, one-way ANOVA was conducted, followed by the post-hoc Tukey test. All results were expressed as mean ± standard deviation. The level of significance was set as $P < 0.05$.

3. Results

3.1. mPEG modification increases the volume retention rates of xenogeneic AAM grafts

The volume retention rates showed a decreasing trend from week 1–12 in all the three groups (Fig. 1a). However, the volume retention rates of the immune-deficient group and xenotransplantation (mPEG-modified) group were noticeably increased compared to the xenotransplantation group at week 4 and 12 (Fig. 1b; $p < 0.05$). The graft weight of the immune-deficient group and xenotransplantation (mPEG-modified) group were noticeably increased compared to the xenotransplantation group at week 12 (Fig. 1c; $p < 0.05$). The adipose structures in the three groups were gradually increased from week 1–12 (Fig. 1d).

3.2. mPEG modification increases Treg cells and decrease Th1 cells in xenogeneic AAM grafts

Immunofluorescence staining of perilipin was carried out to reveal the presence of adipogenesis in the transplanted grafts of the mPEG-modified xenotransplantation and control xenotransplantation groups at week 4 and 12. Treg cell infiltration was observed in the two groups at all time points (Fig. 2a). Quantitative analysis of cell infiltration in the grafts showed a significantly higher counts of Treg cells ($CD4^+$ and Foxp3+) and a significantly lower counts of Th1 cells ($CD4^+$ and IFN-γ+) in the mPEG-modified xenotransplantation group compared to the control xenotransplantation group at week 1, 4 and 12 (Fig. 2b and c; $p < 0.05$).

3.3. mPEG modification increases the adipogenesis by upregulates M2 macrophage expression and M2 macrophage polarisation-associated cytokines in xenogeneic AAM grafts

Immunofluorescence staining showed that M1 and M2 macrophages infiltrated the grafts (Fig. 3a). There were no obvious differences in the M2/M1 macrophage ratios between the mPEG-modified xenotransplantation and control xenotransplantation groups at week 1 ($p > 0.05$). However, at week 4 and 12, a significantly higher M2/M1 macrophage ratio was detected in the mPEG-modified xenotransplantation group than in the control xenotransplantation group (Fig. 3b; $p < 0.05$). The amounts of adipocyte cells in the two groups were increased gradually from week 1–12. At week 12, the number of adipocytes was significantly higher in the mPEG-modified xenotransplantation group than in the control xenotransplantation group (Fig. 3c; $p < 0.05$). Besides, the mRNA levels of IL-10 and TGF-β1 in control xenotransplantation group were significantly downregulated compared to the mPEG-modified xenotransplantation group at week 1 and week 4, respectively (Fig. 3d and f; $p < 0.05$). Meanwhile, the expression levels of IL-10, IL-13 and TGF-β1 in mPEG-modified xenotransplantation group were markedly upregulated compared to the control xenotransplantation group at week 12 (Fig. 3d, e and 3f; $p < 0.001$). The expression of PPAR-γ in the mPEG-modified xenotransplantation group was markedly upregulated compared to that in the control xenotransplantation group at week 4 and 12 (Fig. 3g; $p < 0.05$). Similarly, the expression of CEBP-β was remarkably higher in the mPEG-modified xenotransplantation group than in the control xenotransplantation group at week 12 (Fig. 3h; $p < 0.05$).

3.4. Treg cells are increased in CD28-SA treatment group and decreased in anti-CD25 antibody treatment group

The results of immunofluorescence staining confirmed Treg cell infiltration in the control, CD28-SA treatment and anti-CD25 antibody treatment groups at all time points (Fig. 4a). Notably, the percentage of Treg cells in CD28-SA treatment group was markedly increased compared to those in anti-CD25 antibody treatment and control groups at week 1, 4 and 12 (Fig. 4b; $p < 0.01$). In the circulation, the percentages of Treg cells in CD28-SA treatment group were remarkably higher than those in the other two groups at day 7 ($p < 0.05$). Meanwhile, the percentage of Treg cells in the anti-CD25 antibody treatment group was comparatively lower than that in the control group (Fig. 4c; $p < 0.01$). No significant differences were observed in the levels of Th1, Th2, Th17 and cytotoxic T lymphocytes among the three groups within 30 days of injection (Fig. 4d–g; $p > 0.05$).

3.5. Treg cells induce M2 macrophage expression in xenogeneic AAM grafts

Immunofluorescence staining showed that M1 and M2 macrophages infiltrated the grafts at all time points (Fig. 5a). In the CD28-SA treatment group, the M2/M1 macrophage ratio was significantly higher at week 4 and 12 compared to the other two groups. Meanwhile, the M2/M1 macrophage ratio of control group was relatively higher than that of anti-CD25 antibody treatment group at week 12 (Fig. 5b; $p < 0.05$). The number of adipocytes increased from week 1–12 in the three groups. At week 4 and 12, the number of adipocytes in CD28-SA treatment group was markedly elevated compared to the other two groups ($p < 0.05$). In addition, the number of adipocytes in anti-CD25 antibody treatment group was comparatively lower than that in control group at week 4 and 12 (Fig. 5c; $p < 0.05$). The volume retention rates decreased from week 1–12 in the three groups, and were noticeably higher in the CD28-SA treatment group than in the other two groups (Fig. 5d; $p < 0.05$). The mRNA levels of IL-10 and IL-13 in anti-CD25 antibody treatment group were significantly downregulated compared to CD28-SA treatment group at week 1 and 4 (Fig. 5e and f; $p < 0.01$). Interestingly, the expression of IL-10 was higher in anti-CD25 antibody treatment group than in the other two groups at week 12 (Fig. 5e; $p < 0.001$). The mRNA levels of TGF-β1 in CD28-SA treatment groups were remarkably higher than the other two groups at week 1, 4 and 12 (Fig. 5g; $p < 0.05$). PPAR-γ and CEBP-β levels were upregulated in the CD28-SA treatment group compared to the other two groups at week 4 and 12 (Fig. 5h and i; $p < 0.05$).

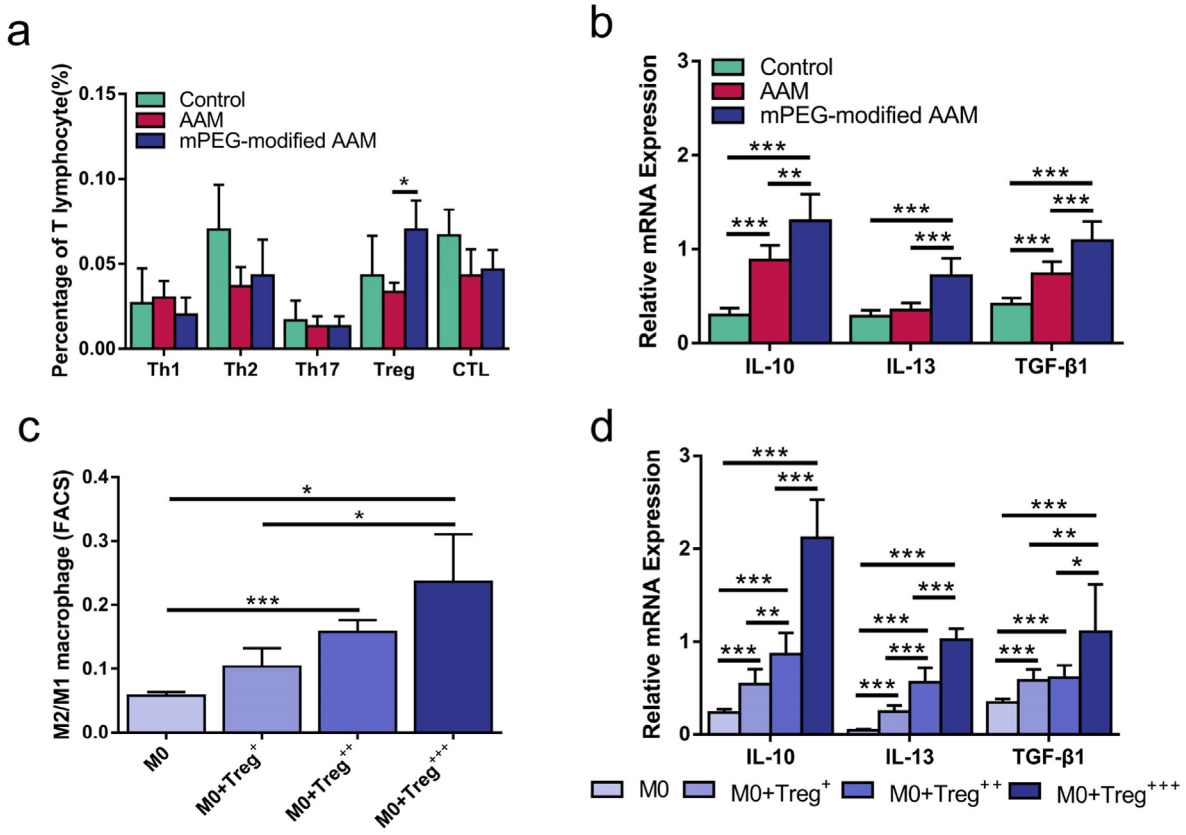

Fig. 6. Results of the lymphocyte co-culture system and the M0-Treg co-culture system. (a) FACS quantification of Th1, Th2, Th17, Treg and cytotoxic T lymphocytes (CTLs) in the lymphocyte co-culture assay at day 3. (b) Relative mRNA expression levels of M2 macrophage polarisation-associated cytokines (IL-10, IL-13 and TGF-β1) in the lymphocyte co-culture assay, as detected by real-time PCR assay. (c) FACS quantification of M2/M1 macrophage (F4/80+, CD11b+, CD11c+, $CD206^{high}$/F480+, CD11b+, CD11c+, $CD206^{low}$) ratio in the co-cultures of M0 macrophages and Treg cells at day 5. (d) Relative mRNA expression levels of M2 macrophage polarisation-associated cytokines (IL-10, IL-13 and TGF-β1) in the M0-Treg co-culture system, as detected by real-time PCR assay. * = $p < 0.05$, ** = $p < 0.01$, *** = $p < 0.001$.

3.6. mPEG modification increases the counts of Treg cells and Treg cells upregulates M2 macrophage expression in vitro

In the lymphocyte co-culture assay, the counts of Treg cells were significantly higher in the mPEG-modified AAM group than in the AAM group (Fig. 6a; $p < 0.05$). However, no obvious differences were found in the levels of Th1, Th2, Th17 and cytotoxic T lymphocytes among the three groups (Fig. 6a; $p > 0.05$). The expression of IL-10, IL-13 and TGF-β1 was higher in mPEG-modified AAM group than in the other two groups (Fig. 6b; $p < 0.001$). In the co-cultures of M0 macrophages and Treg cells in mPEG-modified AAM, it was found that as the Treg cell counts increased, the M2/M1 macrophage ratio (Fig. 6c; $p < 0.05$) and M2 macrophage polarisation-associated cytokine (IL-10, IL-13 and TGF-β1) expression (Fig. 6d; $p < 0.05$) increased.

4. Discussion

Various adipose tissue decellularization methods have been proposed over the past decades [22,31,32]. These decellularization methods have different effects on the preservation of ECM bioactive components and removal of antigen components in AAM [8,9,33]. However, there remains a trade-off between the antigen removal and preservation of native ECM bioactive components. Immunocamouflage modification, rather than the tedious and lengthy chemical/enzymatic treatments, may be a desirable alternative strategy for managing the residual antigens in AAM. Here, we demonstrated that modification of the residual antigens in AAM with mPEG effectively decreased the expression of binding antibodies against residual antigens and the immunogenicity of AAM after xenogeneic transplantation (Supplementary Data 1). More importantly, mPEG modification promoted the regenerative process of AAM *in vivo*. Further analyses revealed that mPEG modification increased the counts of Treg cells and enhanced adipogenesis in the grafts by inducing M2 macrophage polarisation.

The adverse effects of immunogenic antigens may limit the applicability of xenogeneic biomaterials [34,35]. In this study, AAM exhibited better adipogenesis in immune-deficient mice than in wild-type mice. These results indicate that antigen-mediated immune response may adversely affect the *in vivo* adipogenesis of AAM. MCH-I and MCH-II are the membrane proteins and key mediators of transplant rejection [36]. Immune rejection is generally mediated by T cell responses to donor MHC antigens that differ from the recipient (MHC-mismatch) [37]. Foreign MHC molecules activate effector T cells (i.e., Th1 cells) [38], and subsequently proliferate and secrete cytokines (e.g., IFN-γ, IL-2 and TNF-α) [39]. These cytokines can serve as the prominent activation factors for $CD8^+$ cytotoxic T cells and macrophages, which in turn lead to an immune destruction of the graft (e.g., necrosis, degradation and calcification) [36,40]. Therefore, further research should focus on the modification of the residual antigens, especially MHC molecules, in AAMs.

mPEG exerts an immunomodulatory effect by covalently binding with the amino acid residues of foreign antigens, without affecting protein structure [41]. This mPEG modification can form a steric barrier to shield the surface charges and obstruct the interactions between foreign antigens and antigen-presenting cells [42]. Theoretically, mPEG modification can achieve an ideal immunocamouflage effect on AAM. First, AAM is a loose porous collagen scaffold that is conducive to the complete

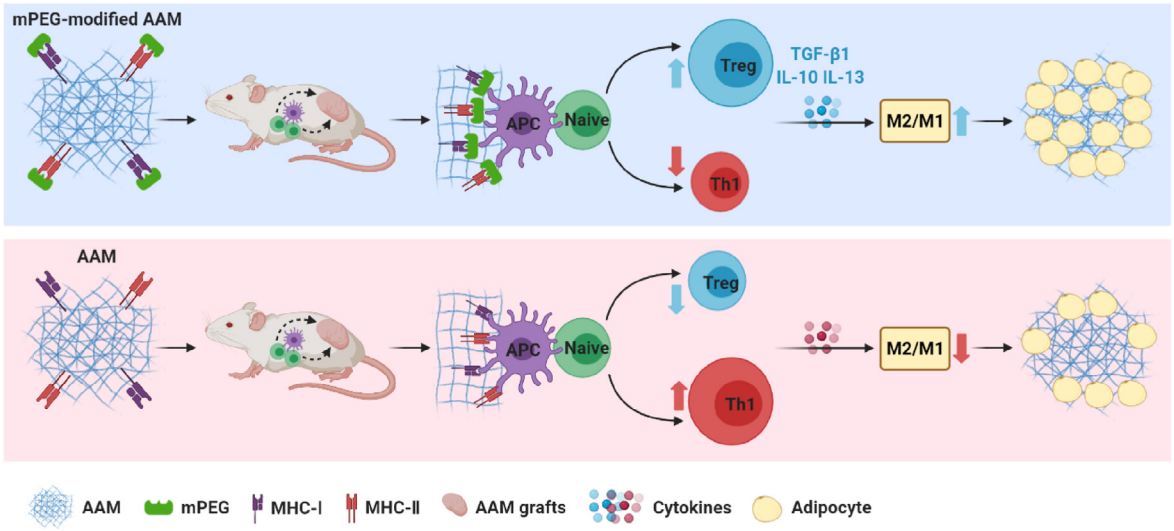

Fig. 7. Model for the adipogenesis mechanism of AAM and mPEG-modified AAM after xenotransplantation. Created with BioRender.com.

infiltration of mPEG solution. Second, the immunogenic MHC molecules located in the broken cell membrane, which retain in the AAM scaffold, are easily modified by mPEG solution. In this study, mPEG modification did not adversely affect cell viability, and the levels of the binding antibodies against MHC-I and MHC-II were decreased in the mPEG-modified AAM (Supplementary Data 1). Moreover, a significantly lower counts of Th1 cells and decreased levels of immunoglobulin in xenogeneic AAM grafts and circulation were detected in the mPEG-modification group compared to the control group (Supplementary Data 1). Taken together, mPEG modification of xenogeneic AAM may serve as an ideal strategy to reduce graft immunogenicity.

Th1 cells are immune effector cells that trigger a T cell-mediated immune response [43], while Treg cells are immune regulatory cells that participate in the maintenance of immune homeostasis [44]. In this study, significantly lower counts of Th1 cells and higher counts of Treg cells were observed in the mPEG-modification group than in the control group. Lymphocyte co-culture assay further showed that Treg cell levels were significantly higher in the mPEG-modified AAM group than in the AAM group. Therefore, we speculate that mPEG modification increases the counts of Treg cells in xenogeneic transplanted AAMs, as demonstrated by the co-culture experiments. Our findings are consistent with those reported by Kang and co-workers [45] showing that mPEG modification prevents the tissue destructive T cell response through the generation/differentiation of functional Treg cells. Other studies also showed that the mPEG-mediated modification of MHC molecules could effectively inhibit or weaken the highly critical cell–cell conjugation and signalling events necessary for immune recognition [24,46]. mPEG-modified antigens (e.g., MHC molecules) often exhibit a reduced affinity for receptors compared to the unmodified antigen [47]. The strength of the interactions between MHC and T cell receptor (TCR) is closely associated with the fate of T cells [48,49]. Low-affinity antigen-TCR engagement can lead to a decrease in intracellular TCR signalling events that enhance the differentiation of naive T cells into Treg cells [49–51]. Therefore, the upregulation of Treg cells in AAM may be attributed to the low-affinity antigen-TCR engagement induced by mPEG modification. However, further studies are warranted to elucidate the exact mechanisms involved in this process.

In addition to their ability to suppress immune rejection, Treg cells have recently been recognised as important cells that promote tissue repair and regeneration [52,53]. Therefore, we speculate that an increase in the counts of Treg cells may contribute to the enhanced adipogenesis in mPEG-modified AAM. In this study, mPEG modification effectively induced Treg cell population and promoted adipogenesis in AAM, while systematic downregulation of Treg cells inhibited adipogenesis in AAM compared to the control. This suggests that adipogenesis in AAM is closely related to the counts of Treg cells. It has been reported that Treg cells could promote tissue repair and regeneration by inducing M2 macrophage polarisation through the secretion of inflammatory cytokines [54]. Moreover, the expression levels of both inflammatory cytokines (IL-10, IL-13 and TGF-β1) and M2 macrophages were obviously higher in the mPEG modification and CD28-SA treatment groups than those in the control and anti-CD25 antibody treatment groups. Co-culture of Treg cells with M0 macrophages in mPEG-modified AAM further showed that Treg cells could promote M2 macrophage polarisation through the secretion of IL-10, IL-13 and TGF-β1. M2 macrophages are key inflammatory cells responsible for wound repair and tissue regeneration. Previous studies showed that M2 macrophages could induce the recruitment and differentiation of endothelial cells as well as stem cells, thereby facilitating tissue repair [55,56]. In adipogenic induction models, M2 macrophage directly contributed to the development of adipose tissues through the promotion of angiogenesis and adipogenesis [57,58]. During adipose tissue regeneration, M2 macrophages could promote preadipocyte survival, stem cell recruitment and vascular remodeling by releasing chemokine ligand 12, matrix metalloprotease 9, platelet-derived growth factor, etc. [59,60]. Collectively, the increased counts of Treg cells in mPEG-modified AAM upregulates M2 macrophage expression, and eventually promotes adipose regeneration in the grafts (Fig. 7).

However, several possible adverse issues of mPEG modified technology and limitations of this study should be concerned. First, high dose use (200 mg/kg in rat model) of PEG can be toxic and cause a significant increased in foamy cells in spleen [61,62]. Second, PEG itself can be immunogenic [63–65] and studies suggested an incidence of anti-PEG antibodies in ~0.2% of the general population [66]. Third, the optimal mPEG incubation time and concentration were not studied. Fourth, the long-term effects of mPEG modification on the tissue remodeling of xenogeneic AAM grafts should be experimentally evaluated in the near future. Fifth, a green adipose decellularization method that releases less harmful chemicals and requires a shorter processing time will be developed in our further study. Sixth, the balance between the decellularization method and the mPEG modified technology should be investigated in the further.

5. Conclusion

The residual antigens in AAM could be camouflaged by mPEG without causing any apparent cytotoxicity. The mPEG-modified AAM exhibited a decreased immunogenicity and increased adipogenesis

compared to the control after xenotransplantation. The mechanisms might be attributed to the increased of the counts Treg cells and elevated M2/M1 macrophage ratio upon mPEG modification. Hence, the mPEG-modified AAM may serve as an ideal biomaterial for xenogeneic adipose tissue construction.

Credit author statement

Kaiyang Liu: Conceptualization, Methodology, Formal analysis, Data curation, Investigation, Resources, Data curation, Writing – original draft. Yunfan He: Conceptualization, Validation, Formal analysis, Writing – review & editing, Project administration. Yao Yao: Validation, Formal analysis, Investigation, Resources. Yuchen Zhang: Investigation, Resources, Visualization. Zihan Cai: Investigation, Resources, Data curation. Jiangjiang Ru: Investigation, Data curation. Xiangdong Zhang: Investigation. Xiaoxuan Jin: Investigation. Mimi Xu: Investigation. Yibao Li: Investigation. Qizhuan Ma: Investigation. Jianhua Gao: Supervision. Feng Lu: Supervision, Project administration, Funding acquisition.

Declaration of competing interest

The authors declare that they have no known competing financial interests or personal relationships that could have appeared to influence the work reported in this paper.

Acknowledgments

This work was supported by the National Nature Science Foundation of China (81772101, 81801933), the Natural Science Foundation of Guangdong Province of China (2017A030313900), and the Administrator Foundation of Nanfang Hospital (2016Z010, 2017C008).

Appendix A. Supplementary data

Supplementary data to this article can be found online at https://doi.org/10.1016/j.mtbio.2021.100161.

References

[1] L. Vaienti, M. Soresina, A. Menozzi, Parascapular free flap and fat grafts: combined surgical methods in morphological restoration of hemifacial progressive atrophy, Plast. Reconstr. Surg. 116 (3) (2005) 699–711, https://doi.org/10.1097/01.prs.0000177449.12366.48.

[2] Y.X. Zhang, T.J. Hayakawa, L.S. Levin, G.G. Hallock, D. Lazzeri, The economy in autologous tissue transfer: Part 1. The kiss flap technique, Plast. Reconstr. Surg. 137 (3) (2016) 1018–1030, https://doi.org/10.1097/01.prs.0000479971.99309.21.

[3] K. Mineda, S. Kuno, H. Kato, K. Kinoshita, K. Doi, I. Hashimoto, H. Nakanishi, K. Yoshimura, Chronic inflammation and progressive calcification as a result of fat necrosis: the worst outcome in fat grafting, Plast. Reconstr. Surg. 133 (5) (2014) 1064–1072, https://doi.org/10.1097/PRS.0000000000000097.

[4] H. Kato, K. Mineda, H. Eto, K. Doi, S. Kuno, K. Kinoshita, K. Kanayama, K. Yoshimura, Degeneration, regeneration, and cicatrization after fat grafting: dynamic total tissue remodeling during the first 3 months, Plast. Reconstr. Surg. 133 (3) (2014) 303e–313e, https://doi.org/10.1097/PRS.0000000000000066.

[5] L. Requena, C. Requena, L. Christensen, U.S. Zimmermann, H. Kutzner, L. Cerroni, Adverse reactions to injectable soft tissue fillers, J. Am. Acad. Dermatol. 64 (1) (2011) 1–34, https://doi.org/10.1016/j.jaad.2010.02.064, quiz 35-6.

[6] C. Yu, J. Bianco, C. Brown, L. Fuetterer, J.F. Watkins, A. Samani, L.E. Flynn, Porous decellularized adipose tissue foams for soft tissue regeneration, Biomaterials 34 (13) (2013) 3290–3302, https://doi.org/10.1016/j.biomaterials.2013.01.056.

[7] J.S. Kim, J.S. Choi, Y.W. Cho, Cell-free hydrogel system based on a tissue-specific extracellular matrix for in situ adipose tissue regeneration, ACS Appl. Mater. Interfaces 9 (10) (2017) 8581–8588, https://doi.org/10.1021/acsami.6b16783.

[8] G. Giatsidis, J. Succar, T.D. Waters, W. Liu, P. Rhodius, C. Wang, T.J. Nilsen, E. Chnari, D.P. Orgill, Tissue-engineered soft-tissue reconstruction using noninvasive mechanical preconditioning and a shelf-ready allograft adipose matrix, Plast. Reconstr. Surg. 144 (4) (2019) 884–895, https://doi.org/10.1097/PRS.0000000000006085.

[9] D.A. Young, D.O. Ibrahim, D. Hu, K.L. Christman, Injectable hydrogel scaffold from decellularized human lipoaspirate, Acta Biomater. 7 (3) (2011) 1040–1049, https://doi.org/10.1016/j.actbio.2010.09.035.

[10] M. Lin, J. Ge, X. Wang, Z. Dong, M. Xing, F. Lu, Y. He, Biochemical and biomechanical comparisions of decellularized scaffolds derived from porcine subcutaneous and visceral adipose tissue, J. Tissue Eng. 10 (2019), https://doi.org/10.1177/2041731419888168, 204173141988816.

[11] L.E. Kokai, B.K. Schilling, E. Chnari, Y.C. Huang, E.A. Imming, A. Karunamurthy, R.K. Khouri, R.A. D'Amico, S.R. Coleman, K.G. Marra, J.P. Rubin, Injectable Allograft adipose matrix supports adipogenic tissue remodeling in the nude mouse and human, Plast. Reconstr. Surg. 143 (2) (2019) 299e–309e, https://doi.org/10.1097/PRS.0000000000005269.

[12] G.S. Hussey, J.L. Dziki, S.F. Badylak, Extracellular matrix-based materials for regenerative medicin, Nat Rev Mater 3 (173) (2018).

[13] A.G. Arroyo, M.L. Iruela-Arispe, Extracellular matrix, inflammation, and the angiogenic response, Cardiovasc. Res. 86 (2) (2010) 226–235, https://doi.org/10.1093/cvr/cvq049.

[14] L. Huleihel, G.S. Hussey, J.D. Naranjo, L. Zhang, J.L. Dziki, N.J. Turner, D.B. Stolz, S.F. Badylak, Matrix-bound nanovesicles within ECM bioscaffolds, Sci Adv 2 (6) (2016), e1600502, https://doi.org/10.1126/sciadv.1600502.

[15] S.W. Lane, D.A. Williams, F.M. Watt, Modulating the stem cell niche for tissue regeneration, Nat. Biotechnol. 32 (8) (2014) 795–803, https://doi.org/10.1038/nbt.2978.

[16] I. Ullah, R. Abu-Dawud, J.F. Busch, A. Rabien, B. Erguen, I. Fischer, P. Reinke, A. Kurtz, VEGF - supplemented extracellular matrix is sufficient to induce endothelial differentiation of human iPSC, Biomaterials 216 (2019) 119283, https://doi.org/10.1016/j.biomaterials.2019.119283.

[17] C. Thomas-Porch, J. Li, F. Zanata, E.C. Martin, N. Pashos, K. Genemaras, J.N. Poche, N.P. Totaro, M.R. Bratton, D. Gaupp, T. Frazier, X. Wu, L.M. Ferreira, W. Tian, G. Wang, B.A. Bunnell, L. Flynn, D. Hayes, J.M. Gimble, Comparative proteomic analyses of human adipose extracellular matrices decellularized using alternative procedures, J. Biomed. Mater. Res. 106 (9) (2018) 2481–2493, https://doi.org/10.1002/jbm.a.36444.

[18] J.Q. Wang, J. Fan, J.H. Gao, C. Zhang, S.L. Bai, Comparison of in vivo adipogenic capabilities of two different extracellular matrix microparticle scaffolds, Plast. Reconstr. Surg. 131 (2) (2013) 174e–187e, https://doi.org/10.1097/PRS.0b013e3182789bb2.

[19] A. Mirzarafie, R.K. Grainger, B. Thomas, W. Bains, F.I. Ustok, C.R. Lowe, A fast and mild decellularization protocol for obtaining extracellular matrix, Rejuvenation Res. 17 (2) (2014) 159–160, https://doi.org/10.1089/rej.2013.1488.

[20] P.M. Crapo, T.W. Gilbert, S.F. Badylak, An overview of tissue and whole organ decellularization processes, Biomaterials 32 (12) (2011) 3233–3243, https://doi.org/10.1016/j.biomaterials.2011.01.057.

[21] B.N. Brown, J.M. Freund, L. Han, J.P. Rubin, J.E. Reing, E.M. Jeffries, M.T. Wolf, S. Tottey, C.A. Barnes, B.D. Ratner, S.F. Badylak, Comparison of three methods for the derivation of a biologic scaffold composed of adipose tissue extracellular matrix, Tissue Eng. C Methods 17 (4) (2011) 411–421, https://doi.org/10.1089/ten.TEC.2010.0342.

[22] M. Kawecki, W. Labus, A. Klama-Baryla, D. Kitala, M. Kraut, J. Glik, M. Misiuga, M. Nowak, T. Bielecki, A. Kasperczyk, A review of decellurization methods caused by an urgent need for quality control of cell-free extracellular matrix' scaffolds and their role in regenerative medicine, J. Biomed. Mater. Res. B Appl. Biomater. 106 (2) (2018) 909–923, https://doi.org/10.1002/jbm.b.33865.

[23] S.P. Hoo, Q.L. Loh, Z. Yue, J. Fu, T. Tan, C. Choong, P. Chan, Preparation of a soft and interconnected macroporous hydroxypropyl cellulose methacrylate scaffold for adipose tissue engineering, J. Mater. Chem. B 1 (24) (2013) 3107–3117, https://doi.org/10.1039/c3tb00446e.

[24] D.L. Kyluik-Price, M.D. Scott, Effects of methoxypoly (Ethylene glycol) mediated immunocamouflage on leukocyte surface marker detection, cell conjugation, activation and alloproliferation, Biomaterials 74 (2016) 167–177, https://doi.org/10.1016/j.biomaterials.2015.09.047.

[25] Y. Le, W.M. Toyofuku, M.D. Scott, Immunogenicity of murine mPEG-red blood cells and the risk of anti-PEG antibodies in human blood donors, Exp. Hematol. 47 (2017) 36–47, https://doi.org/10.1016/j.exphem.2016.11.001, e2.

[26] S.N.S. Alconcel, A.S. Baas, H.D. Maynard, FDA-approved poly(ethylene glycol)–protein conjugate drugs, Polym Chem-Uk 2 (7) (2011) 1442, https://doi.org/10.1039/c1py00034a.

[27] Y. Le, M.D. Scott, Immunocamouflage: the biophysical basis of immunoprotection by grafted methoxypoly(ethylene glycol) (mPEG), Acta Biomater. 6 (7) (2010) 2631–2641, https://doi.org/10.1016/j.actbio.2010.01.031.

[28] Y. Teramura, H. Iwata, Surface modification of islets with PEG-lipid for improvement of graft survival in intraportal transplantation, Transplantation 88 (5) (2009) 624–630, https://doi.org/10.1097/TP.0b013e3181b230ac.

[29] S. Wang, L. Li, Y. Liu, C. Li, M. Zhang, B. Wang, Z. Huang, X. Gao, Z. Wang, Treatment with mPEG-SPA improves the survival of corneal grafts in rats by immune camouflage, Biomaterials 43 (2015) 13–22, https://doi.org/10.1016/j.biomaterials.2014.12.001.

[30] Y. He, M. Lin, X. Wang, J. Guan, Z. Dong, F. Lu, M. Xing, C. Feng, X. Li, Optimized adipose tissue engineering strategy based on a neo-mechanical processing method, Wound Repair Regen. 26 (2) (2018) 163–171, https://doi.org/10.1111/wrr.12640.

[31] J.K. Wang, B. Luo, V. Guneta, L. Li, S. Foo, Y. Dai, T. Tan, N.S. Tan, C. Choong, M. Wong, Supercritical carbon dioxide extracted extracellular matrix material from adipose tissue, Mater Sci Eng C Mater Biol Appl 75 (2017) 349–358, https://doi.org/10.1016/j.msec.2017.02.002.

[32] J. Dong, M. Yu, Y. Zhang, Y. Yin, W. Tian, Recent developments and clinical potential on decellularized adipose tissue, J. Biomed. Mater. Res. 106 (9) (2018) 2563–2574, https://doi.org/10.1002/jbm.a.36435.

[33] A.E. Turner, C. Yu, J. Bianco, J.F. Watkins, L.E. Flynn, The performance of decellularized adipose tissue microcarriers as an inductive substrate for human adipose-derived stem cells, Biomaterials 33 (18) (2012) 4490–4499, https://doi.org/10.1016/j.biomaterials.2012.03.026.

[34] D.A. Banyard, V. Borad, E. Amezcua, G.A. Wirth, G.R. Evans, A.D. Widgerow, Preparation, characterization, and clinical implications of human decellularized adipose tissue extracellular matrix (hDAM): a comprehensive review, Aesthetic Surg. J. 36 (3) (2016) 349–357, https://doi.org/10.1093/asj/sjv170.
[35] T.J. Keane, S.F. Badylak, The host response to allogeneic and xenogeneic biological scaffold materials, J Tissue Eng Regen Med 9 (5) (2015) 504–511, https://doi.org/10.1002/term.1874.
[36] M.H. Sayegh, L.A. Turka, The role of T-cell costimulatory activation pathways in transplant rejection, N. Engl. J. Med. 338 (25) (1998) 1813–1821, https://doi.org/10.1056/NEJM199806183382506.
[37] H. Shegarfi, O. Reikeras, Review article: bone transplantation and immune response, J. Orthop. Surg. 17 (2) (2009) 206–211, https://doi.org/10.1177/230949900901700218.
[38] S.L. Hargrave, C. Hay, J. Mellon, E. Mayhew, J.Y. Niederkorn, Fate of MHC-matched corneal allografts in Th1-deficient hosts, Invest. Ophthalmol. Vis. Sci. 45 (4) (2004) 1188–1193, https://doi.org/10.1167/iovs.03-0515.
[39] L. Ma, H. Zhang, K. Hu, G. Lv, Y. Fu, D.A. Ayana, P. Zhao, Y. Jiang, The imbalance between Tregs, Th17 cells and inflammatory cytokines among renal transplant recipients, BMC Immunol. 16 (2015) 56, https://doi.org/10.1186/s12865-015-0118-8.
[40] B.N. Brown, J.E. Valentin, A.M. Stewart-Akers, G.P. McCabe, S.F. Badylak, Macrophage phenotype and remodeling outcomes in response to biologic scaffolds with and without a cellular component, Biomaterials 30 (8) (2009) 1482–1491, https://doi.org/10.1016/j.biomaterials.2008.11.040.
[41] E. Hamed, T. Xu, S. Keten, Poly(ethylene glycol) conjugation stabilizes the secondary structure of alpha-helices by reducing peptide solvent accessible surface area, Biomacromolecules 14 (11) (2013) 4053–4060, https://doi.org/10.1021/bm401164t.
[42] N.A. Rossi, I. Constantinescu, D.E. Brooks, M.D. Scott, J.N. Kizhakkedathu, Enhanced cell surface polymer grafting in concentrated and nonreactive aqueous polymer solutions, J. Am. Chem. Soc. 132 (10) (2010) 3423–3430, https://doi.org/10.1021/ja909174x.
[43] H. Krook, A. Hagberg, Z. Song, U. Landegren, L. Wennberg, O. Korsgren, A distinct Th1 immune response precedes the described Th2 response in islet xenograft rejection, Diabetes 51 (1) (2002) 79–86, https://doi.org/10.2337/diabetes.51.1.79.
[44] S. Wang, J. Jiang, Q. Guan, Z. Lan, H. Wang, C.Y. Nguan, A.M. Jevnikar, C. Du, Reduction of Foxp3-expressing regulatory T cell infiltrates during the progression of renal allograft rejection in a mouse model, Transpl. Immunol. 19 (2) (2008) 93–102, https://doi.org/10.1016/j.trim.2008.03.004.
[45] N. Kang, W.M. Toyofuku, X. Yang, M.D. Scott, Inhibition of allogeneic cytotoxic T cell (CD8(+)) proliferation via polymer-induced Treg (CD4(+)) cells, Acta Biomater. 57 (2017) 146–155, https://doi.org/10.1016/j.actbio.2017.04.025.
[46] D. Wang, W.M. Toyofuku, A.M. Chen, M.D. Scott, Induction of immunotolerance via mPEG grafting to allogeneic leukocytes, Biomaterials 32 (35) (2011) 9494–9503, https://doi.org/10.1016/j.biomaterials.2011.08.061.
[47] R. Webster, E. Didier, P. Harris, N. Siegel, J. Stadler, L. Tilbury, D. Smith, PEGylated proteins: evaluation of their safety in the absence of definitive metabolism studies, Drug Metab. Dispos. 35 (1) (2007) 9–16, https://doi.org/10.1124/dmd.106.012419.
[48] C. Kim, M.A. Williams, Nature and nurture: T-cell receptor-dependent and T-cell receptor-independent differentiation cues in the selection of the memory T-cell pool, Immunology 131 (3) (2010) 310–317, https://doi.org/10.1111/j.1365-2567.2010.03338.x.
[49] S.Z. Josefowicz, L.F. Lu, A.Y. Rudensky, Regulatory T cells: mechanisms of differentiation and function, Annu. Rev. Immunol. 30 (2012) 531–564, https://doi.org/10.1146/annurev.immunol.25.022106.141623.
[50] S. Sauer, L. Bruno, A. Hertweck, D. Finlay, M. Leleu, M. Spivakov, Z.A. Knight, B.S. Cobb, D. Cantrell, E. O'Connor, K.M. Shokat, A.G. Fisher, M. Merkenschlager, T cell receptor signaling controls Foxp3 expression via PI3K, Akt, and mTOR, Proc. Natl. Acad. Sci. U. S. A. 105 (22) (2008) 7797–7802, https://doi.org/10.1073/pnas.0800928105.
[51] M.S. Turner, L.P. Kane, P.A. Morel, Dominant role of antigen dose in CD4+Foxp3+ regulatory T cell induction and expansion, J. Immunol. 183 (8) (2009) 4895–4903, https://doi.org/10.4049/jimmunol.0901459.
[52] C. Raffin, L.T. Vo, J.A. Bluestone, Treg cell-based therapies: challenges and perspectives, Nat. Rev. Immunol. 20 (3) (2020) 158–172, https://doi.org/10.1038/s41577-019-0232-6.
[53] D.M. Zaiss, C.M. Minutti, J.A. Knipper, Immune- and non-immune-mediated roles of regulatory T-cells during wound healing, Immunology 157 (3) (2019) 190–197, https://doi.org/10.1111/imm.13057.
[54] J. Weirather, U.D. Hofmann, N. Beyersdorf, G.C. Ramos, B. Vogel, A. Frey, G. Ertl, T. Kerkau, S. Frantz, Foxp3+ CD4+ T cells improve healing after myocardial infarction by modulating monocyte/macrophage differentiation, Circ. Res. 115 (1) (2014) 55–67, https://doi.org/10.1161/CIRCRESAHA.115.303895.
[55] M. Kloc, R.M. Ghobrial, J. Wosik, A. Lewicka, S. Lewicki, J.Z. Kubiak, Macrophage functions in wound healing, J Tissue Eng Regen Med 13 (1) (2019) 99–109, https://doi.org/10.1002/term.2772.
[56] T.A. Wynn, K.M. Vannella, Macrophages in tissue repair, regeneration, and fibrosis, Immunity 44 (3) (2016) 450–462, https://doi.org/10.1016/j.immuni.2016.02.015.
[57] T.T. Han, S. Toutounji, B.G. Amsden, L.E. Flynn, Adipose-derived stromal cells mediate in vivo adipogenesis, angiogenesis and inflammation in decellularized adipose tissue bioscaffolds, Biomaterials 72 (2015) 125–137, https://doi.org/10.1016/j.biomaterials.2015.08.053.
[58] Z. Li, F. Xu, Z. Wang, T. Dai, C. Ma, B. Liu, Y. Liu, Macrophages undergo M1-to-M2 transition in adipose tissue regeneration in a rat tissue engineering model, Artif. Organs 40 (10) (2016) E167–E178, https://doi.org/10.1111/aor.12756.
[59] J. Cai, J. Feng, K. Liu, S. Zhou, F. Lu, Early macrophage infiltration improves fat graft survival by inducing angiogenesis and hematopoietic stem cell recruitment, Plast. Reconstr. Surg. 141 (2) (2018) 376–386, https://doi.org/10.1097/PRS.0000000000004028.
[60] K.L. Spiller, R.R. Anfang, K.J. Spiller, J. Ng, K.R. Nakazawa, J.W. Daulton, G. Vunjak-Novakovic, The role of macrophage phenotype in vascularization of tissue engineering scaffolds, Biomaterials 35 (15) (2014) 4477–4488, https://doi.org/10.1016/j.biomaterials.2014.02.012.
[61] T. Kawaguchi, T. Honda, M. Nishihara, T. Yamamoto, M. Yokoyama, Histological study on side effects and tumor targeting of a block copolymer micelle on rats, J. Contr. Release 136 (3) (2009) 240–246, https://doi.org/10.1016/j.jconrel.2009.02.011.
[62] K. Shiraishi, M. Yokoyama, Toxicity and immunogenicity concerns related to PEGylated-micelle carrier systems: a review, Sci. Technol. Adv. Mater. 20 (1) (2019) 324–336, https://doi.org/10.1080/14686996.2019.1590126.
[63] T. Cheng, P. Wu, M. Wu, J. Chern, S.R. Roffler, Accelerated clearance of polyethylene glycol-modified proteins by anti-polyethylene glycol IgM, Bioconjugate Chem. 10 (3) (1999) 520–528, https://doi.org/10.1021/bc980143z.
[64] R.P. Garay, R. El-Gewely, J.K. Armstrong, G. Garratty, P. Richette, Antibodies against polyethylene glycol in healthy subjects and in patients treated with PEG-conjugated agents, Expet Opin. Drug Deliv. 9 (11) (2012) 1319–1323, https://doi.org/10.1517/17425247.2012.720969.
[65] J.K. Armstrong, G. Hempel, S. Koling, L.S. Chan, T. Fisher, H.J. Meiselman, G. Garratty, Antibody against poly(ethylene glycol) adversely affects PEG-asparaginase therapy in acute lymphoblastic leukemia patients, Cancer-Am Cancer Soc 110 (1) (2007) 103–111, https://doi.org/10.1002/cncr.22739.
[66] A.W. Richter, E. Akerblom, Polyethylene glycol reactive antibodies in man: titer distribution in allergic patients treated with monomethoxy polyethylene glycol modified allergens or placebo, and in healthy blood donors, Int. Arch. Allergy Appl. Immunol. 74 (1) (1984) 36–39, https://doi.org/10.1159/000233512.